International Journal of Technology (2017) 8: 1445-1454
ISSN 2086-9614

CRYSTAL -GROWTH KINETICS OF MAGNETITE (Fe_3O_4) NANOPARTICLES USING THE OSTWALD RIPENING MODEL

Ahmad Fadli[1*], Amun Amri[1], Esty Octiana Sari[1], Iwantono[2], Arisman Adnan[3]

[1]*Department of Chemical Engineering, Faculty of Engineering, Universitas Riau, Jl. HR Subrantas Km 12.5 Pekanbaru 28293, Riau, Indonesia*
[2]*Department of Physics, Faculty of Mathematics and Natural Sciences, Universitas Riau, Jl. HR Subrantas Km 12.5 Pekanbaru 28293, Riau, Indonesia*
[3]*Department of Mathematics, Faculty of Mathematics and Natural Sciences, Universitas Riau, Jl. HR Subrantas Km 12.5 Pekanbaru 28293, Riau, Indonesia*

(Received: March 2017 / Revised: April 2017 / Accepted: November 2017)

ABSTRACT

Magnetite nanoparticles (Fe_3O_4) are a type of magnetic particle with huge potential for application as a drug carrier due to their excellent superparamagnetic, biocompatible, and easily modified surface properties. One characteristic of nanoparticles is that they can be controlled by studying the evolution of crystal growth. The purpose of this research is to study the evolution of magnetite-crystal growth and determine the crystal growth kinetics using the Ostwald ripening model. Magnetite nanoparticles were synthesized from $FeCl_3$, citrate, urea, and polyethylene glycol using the hydrothermal method at 220^{o}C for times ranging from 1–12 hours. The characterizations using X-ray diffraction (XRD) indicated that the magnetite began to form after 3 hours synthesis. The crystallinity and crystal size of the magnetite increased with the reaction time. The diameter size of the magnetite crystals was in the range of 10–29 nm. The characterizations using a transmission electron microscope (TEM) showed that magnetite nanoparticles had a relatively uniform size and were not agglomerated. The core-shell nanoparticles were obtained after 3 hours synthesis and had a diameter of 60 nm, whereas the irregular-shaped nanoparticles were obtained in 12 hours and had a diameter of 50 nm. The characterizations using a vibrating sample magnetometer (VSM) revealed that magnetite nanoparticles have superparamagnetic properties. The magnetization saturation (Ms) value was proportional to the degree of crystallinity. The magnetite-crystal growth data can be fitted to an Ostwald ripening model with the growth controlled by the dissolution of the surface reaction ($n \approx 4$).

Keywords: Crystal growth; Hydrothermal; Magnetite; Nanoparticles; Ostwald ripening

1. INTRODUCTION

In recent times, nanoparticle technology has become a new trend in the biomedical world. One application of nanoparticles is in a drug delivery system. Nano drug delivery is a method for delivering a drug directly in the target therapies. This method was proposed by Paul Ehrlich, who received the Nobel Prize in Medicine in 1908. The principle of this method is that the drug is conjugated into nanoparticles, which act as a as drug carrier, and then injected into a vein. Furthermore, where the drug carrier has superparamagnetic properties, the delivery to the target cell is controlled by an external magnetic field. The advantages of nano drug delivery compared

*Corresponding author's email: fadliunri@yahoo.com, Tel: +62-761-566-937, Fax: +62-761-566-937
Permalink/DOI: https://doi.org/10.14716/ijtech.v8i8.738

to conventional medication methods are: (1) it has the ability to treat the specific targets in the body; (2) the dose of the drug is reduced; (3) the concentration of the drug at the nontarget sites is reduced; and (4) the side effects caused by drug toxicity in cells/nontarget tissues are reduced (Arruebo et al., 2007).

A crucial issue in the development of nano-drug-delivery technology is the state of emergency caused by cancer being the second highest cause of death in the world. World Health Organization (WHO) figures, if this is not controlled, an estimated 26 million people will suffer from cancer and 17 million will die of cancer in 2030 (The Union for International Cancer Control's (Union Internationale Contre le Cancer, UICC, 2009). Meanwhile, the chemotherapy that is commonly used is less effective because it is not only deadly for cancer cells but also for healthy cells. Nano drug delivery is a method that promises to be the solution for the various side effects caused by chemotherapy.

The magnetite nanoparticle (Fe_3O_4) is one of the materials that is a very promising candidate for being applied to drug delivery due to its superparamagnetic and high-biocompatibility properties (Mohapatra & Anand, 2010). Many techniques have been developed to produce nanoparticles, including the hydrothermal (Cheng et al., 2010), sonochemistry (Khalil et al., 2017), and combined destruction (Fitriana et al., 2017) techniques. Nanomagnetite has been used as a contrast agent in magnetic resonance imaging (MRI) and hyperthermia for cancer therapy (Qiao et al., 2009). Cheng et al. (2010) synthesized nanomagnetite for use as a drug delivery system, which was made from $FeCl_3$, citrate, urea, and polyacrylamide (PAM) using the hydrothermal method at 200^oC. The resulting magnetite particles were hollow-shell shaped, the core was superparamagnetic, it had high solubility in water, and was ideal for applying in drug delivery. With these superior characteristics, it will be better if the size and morphology of the particles can be controlled because it is a critical factor in drug delivery systems. The size and morphology of the particles used in drug delivery affect accessibility and the time of residence in the bloodstream (Bae & Park, 2011; Yu et al., 2012).

The study of the evolution of crystal growth can help with understanding the factors that influence the growth of crystals. An understanding of the factors that affect crystal growth kinetics and microstructure development in nanocrystals is fundamental to the control of nanoparticle properties. It is important for the process of tailoring the nanoparticles to have uniform size and morphology (Hwang et al., 2012). This research was carried out by modeling the crystal growth kinetics of magnetite nanoparticles using the Ostwald ripening model. In this study, the biocompatibility of the nanoparticles was also improved by using the capping agent polyethylene glycol (PEG). PEG is a hydrophilic polymer that is stable, has a high biocompatibility, and is widely used in drug delivery applications. Thus, from this study it is expected that biocompatible, superparamagnetic magnetite nanoparticles with a controlled size and morphology that meet the criteria for application in drug delivery can be obtained.

2. METHODOLOGY

This study consisted of three main stages: (1) the preparation of magnetite nanoparticles from the starting material $FeCl_3$ using the hydrothermal method; (2) characterization with a transmission electron microscope (TEM), X-ray diffraction (XRD), and a magnetometer; and (3) modeling the kinetics of magnetite-crystal growth.

2.1. Synthesis of Magnetite Nanoparticles

The magnetite nanoparticles were synthesized using the hydrothermal method. A total of 2 mmol $FeCl_3$ (0.05M), 4 mmol of sodium citrate (0.10 M), and 6 mmol of urea (0.15M) was dissolved into 40 mL of distilled water, then 0.38 g PEG (7.5 g / L) was added until it completely dissolved, and the solution was finally transferred into a Teflon-lined autoclave. The

Teflon-lined autoclave was put into an oven and the temperature was set to 220°C. The reaction times used in this study were 1, 2, 3, 5, 7, 9, and 12 hours. The black precipitate that formed was separated by a bar magnet, then washed with water and ethanol, and dried at 60°C overnight.

2.2. XRD Characterization

The crystallinity, composition, and size of the nanoparticles were determined using XRD. Approximately 200 mg of the sample was placed directly onto a piece of aluminum measuring 2×2.5 cm. The samples were characterized using an XRD instrument with Cu radiation light (λ = 1.54 Å), a voltage of 40 kV, and a current of 30 Ma at 2θ 10−99.97°.

2.3. TEM Characterization

The size, morphology, and aggregate of the particles were analyzed using a TEM microscope (TEM JEOL JEM 1400) operated at 5 kV under vacuum.

2.4. VSM Characterization

The characteristics of the magnetic nanoparticles were analyzed using a vibrating sample magnetometer (VSM) of type VSM1.2H Oxford. The magnetization curves were measured at room temperature with a magnetic field that varied in the range of -1 to 1 Tesla.

2.5. Kinetic Modeling of Crystal Growth

The Ostwald ripening model is a classical model of crystal growth that describes the "change of particle size" phenomenon. It is based on the growth of larger particles from smaller particles. The driving force for this process is the total reduction of surface free energy based on the Gibbs-Thomson equation. The equilibrium concentration of the solute on the surface of the larger particles is lower than for the smaller particles, and results in a concentration gradient that causes the solute ions to move from the small particles to the larger particles. The Ostwald ripening model assumes that the crystal growth mechanism is applicable to all length scales. It is also claimed that the application of this method to the estimation of diffusion coefficients is valid for any colloidal system that is characterized by a small particle size distribution at all stages of its growth (Thanh et al., 2014). Although there has been no kinetic modeling of crystal growth for magnetite nanoparticles, this model is commonly used in the study of early crystal growth. The general equation of the Ostwald ripening model is presented in Equation 1.

$$(r - r_0)^n = Kt \tag{1}$$

where r is crystal radius, r_o is the radius of the crystal formed initially, K is constant, and t is the time of reaction. Equation 1 was then converted into the following equation:

$$\ln(r - r_0) = LnK + \frac{1}{n}\ln(t - t_0) \tag{2}$$

Based on the intercept and slope, k and n were obtained. Furthermore, the values of r and ro were obtained from the model curve. The curve obtained from the experiment matched the kinetic curve for the Ostwald ripening model.

3. RESULTS AND DISCUSSION

3.1. Synthesis and Characterization of Magnetite Nanoparticles

Magnetite nanoparticles were synthesized using the hydrothermal method. The reactants used were $FeCl_3$, urea, and sodium citrate. PEG was added as the capping agent and to increase biocompatibility to make the particles suitable for drug delivery (Arruebo et al., 2007; Cao et al., 2012; Yu et al., 2012). Since Fe_3O_4 crystal consists of Fe^{3+} and Fe^{2+}, it would require a

reducing agent to reduce Fe $^{3+}$ to become Fe $^{2+}$. Citrate was used as the reductor to make Fe^{3+} become Fe^{2+} at a high temperature (Equation 3). Citrate also can make complexes with Fe^{3+} and Fe^{2+}; these complexes reduce the number of free ions and produce a slow reaction, which is the best way to form crystals (Cheng et al., 2010). A high temperature causes the hydrolysis of urea in alkaline conditions (Equation 4). The basic conditions supported the formation of Fe (II) hydroxide and Fe (III) hydroxide (Equations 5 and 6), then the magnetite was formed by the reaction between one molecule of Fe (II) hydroxide and two molecules of Fe (III) hydroxide (Equation 6).

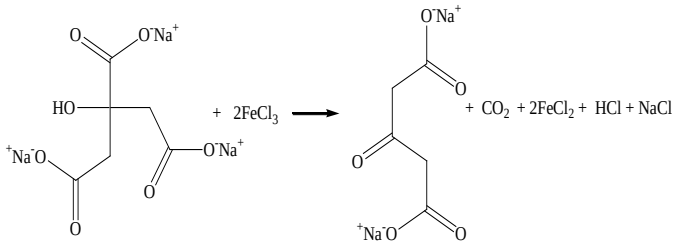

(3)

$$(NH_2)_2CO_{(aq)} + 3H_2O_{(aq)} \rightarrow 2NH_4OH_{(aq)} + CO_{2(g)} \quad (4)$$

$$Fe^{2+}_{(aq)} + 2\,NH_4OH_{(aq)} \rightarrow Fe(OH)_{2(s)} + 2NH_4^+{}_{(aq)} \quad (5)$$

$$Fe^{3+}_{(aq)} + 3\,NH_4OH_{(aq)} \rightarrow Fe(OH)_{3(s)} + 3NH_4^+{}_{(aq)} \quad (6)$$

$$Fe(OH)_{2(s)} + 2Fe(OH)_{3(s)} \rightarrow Fe_3O_{4(s)} + 4H_2O_{(aq)} \quad (7)$$

The formation of magnetite nanoparticles with black precipitate is as depicted in Figure 1. The precipitate was thoroughly dispersed in water. The presence of PEG that has an -OH group on the surface of the nanoparticles makes the nanoparticles hydrophilic and negatively charged. Thus, the nanoparticles have a longer time of residence in the bloodstream (high bioavailability) because this corresponds to the nature of the plasma proteins, which are also hydrophilic and negatively charged. In general, phagocytosis will occur in particles that are non-polar (hydrophobic) and positively charged, as they are considered to be a substance that is foreign to the body. When brought closer to the external magnetic field, the precipitate interacts with the magnetic field and is attracted completely after 45 seconds. The magnetic properties of the precipitate appear when exposed to the external magnetic field and then disappear when the magnetic field is removed. This shows that magnetite nanoparticles have paramagnetic properties.

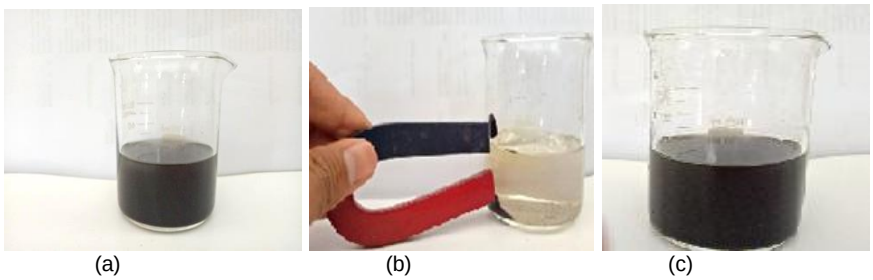

(a) (b) (c)

Figure 1 The as-synthesized black precipitate well dispersed in water (a), the precipitate interacts with the external magnetic field and is attracted completely after 45 seconds (b), and the re-dispersal of the powder in the water after the magnetic field is removed (c)

Figure 2 demonstrates that after 1 hour and 2 hours of synthesis there was no precipitate. The solution was still yellow after 1 hour of synthesis and turned brown after 2 hours of synthesis. The precipitate began to form at 3 hours of synthesis. The precipitate color darkened as the time of synthesis increased.

(a) (b) (c) (d) (e)

Figure 2 The as-synthesized product at 1 (a), 2 (b), 3 (c), 5 (d), and 12 hours (e)

3.1.1. XRD characterization result

The XRD patterns match the standard pattern for Fe_3O_4, with the highest intensity at 2Θ 35.54°, 57.06°, and 62.66°, which confirms that the precipitate was pure magnetite. The intensity of the peak rose as the time of synthesis increased, which indicates that the crystallinity of the magnetite nanoparticles also was amplified.

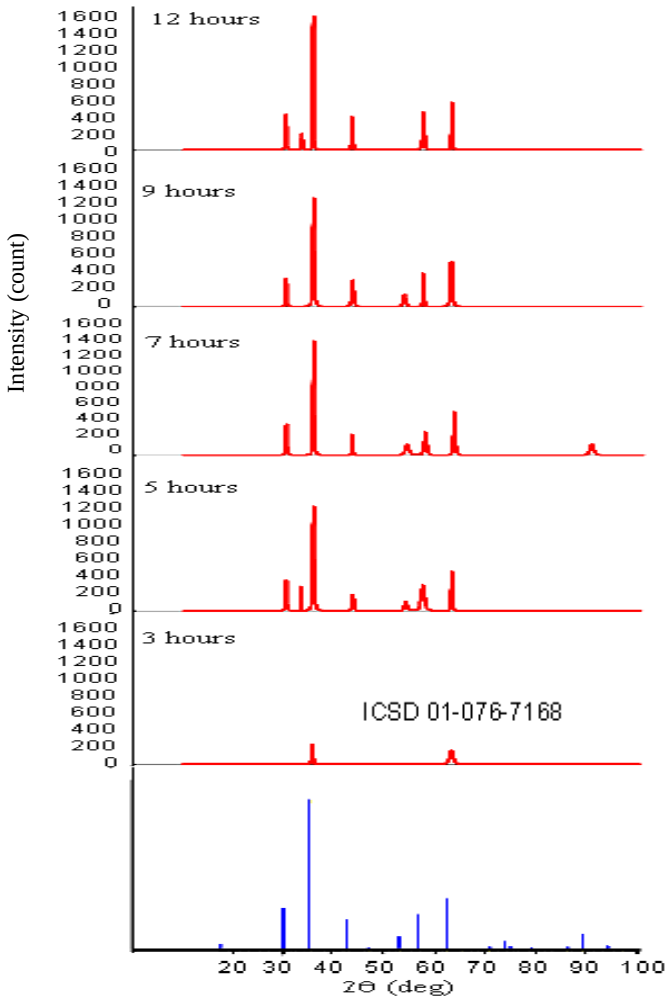

Figure 3 The XRD pattern of as-synthesized magnetite at 220°C for 3, 5, 7, 9, and 12 hours

3.1.2. Magnetic properties characterization result

The magnetic hysteresis curve of magnetite is depicted in Figure 4. There is a very narrow hysteresis loop with a coercivity (Hc) value near zero (0.02 T). This indicates that the as-synthesized nanomagnetite has superparamagnetic properties. A narrow hysteresis loop reveals the very lowest amount of energy lost and the ease of magnetization (Marolt, 2014). This means the synthesized Fe_3O_4 is not only suitable for use as a drug carrier but is also very promising for being applied as a recording medium, and in data storage and supercapacitors.

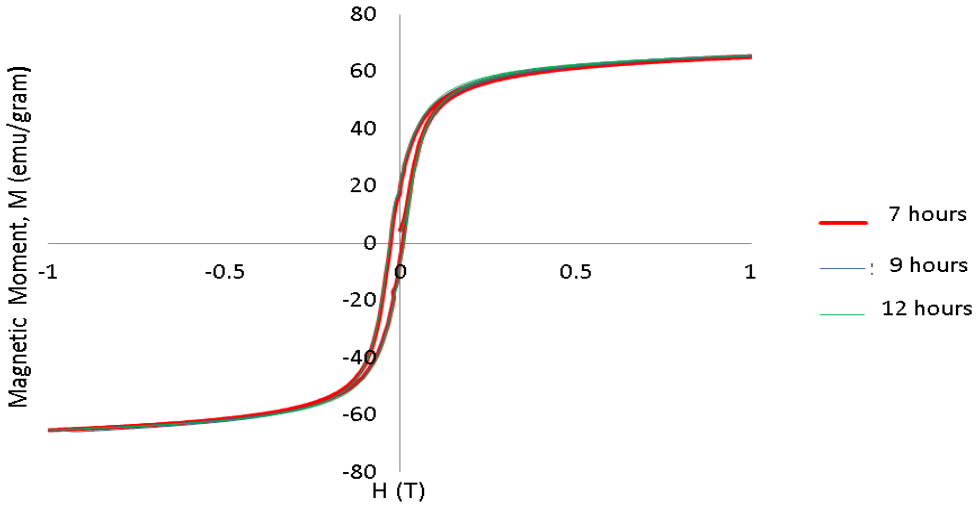

Figure 4 The hysteresis curves of as-synthesized magnetite nanoparticles

The magnetization saturation values are detailed in Table 1. The magnetization saturation is the maximum magnetization or the conditions under which a further increase in the magnetic field intensity (H) is not going to cause a rise in the density of the magnetic field (M). The resulting saturation magnetization is relatively stable each time the synthesis is performed, and is 65 emu/g, and there is a slightly raised saturation magnetization value as the time of synthesis increases. This trend also corresponds to the crystallinity trends (Figure 3 and Table 1). Thus, it can be concluded that the saturation magnetization (Ms) is proportional to the degree of crystallinity of the nanoparticles. When the crystallinity increased, the saturation magnetization increased as well. This is due to the high crystallinity; the structure is similar to the crystal structure of the bulk material.

Table 1 The values for the magnetization saturation and highest intensity peak of the as-synthesized nanomagnetite at 7, 9, and 12 hours

Synthesis time (hours)	Magnetic saturation (emu/g)	Highest intensity of XRD peak (count)
7	65.04	1,330,228
9	65.29	1,384,059
12	65.41	1,490,334

3.1.3.. Morphology characterization result

The morphology of the nanoparticles is revealed in the TEM images (Figure 5), which show that nano-sized particles formed with a uniform size distribution (monodispersity) and were not agglomerated. A synthesis of 3 hours resulting in core-shell-shaped magnetite nanoparticles with a diameter about 60 nm as depicted in Figure 5a. The core section is darker than the shell, indicating high crystallinity in the core section and amorphousness in shell section. The core-

shell structure has advantages for use as a drug carrier. The shell protects the core part from oxidation by the outside air, and serves as an attachment for ligands or drugs (Luszczyk et al., 2014). However, the particles resulting from 12 hours of synthesis have a less regulated morphology and are denser, with diameter of about 50 nm, as depicted in Figure 5b. Thus, the TEM image confirms that the addition of PEG was able to prevent agglomeration among the nanoparticles. The size of nanomagnetite particles that is required to meet the criteria for drug delivery is 10–200 nm.

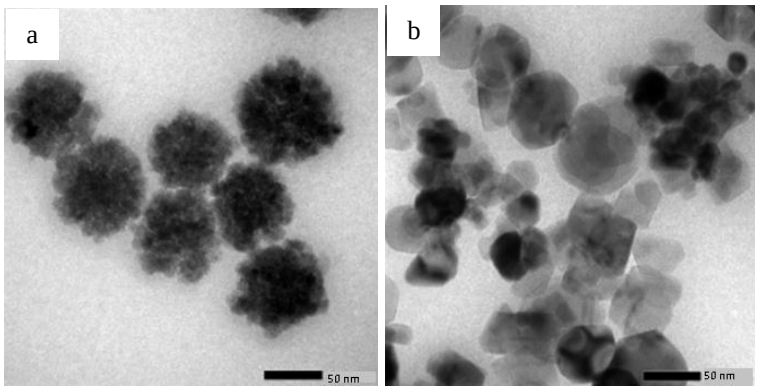

Figure 5 The TEM image of as-synthesized magnetite after 3 hours (a) and 12 hours (b) synthesis time

3.2. Magnetite Nanoparticles Crystal Growth Modeling

The modeling of the magnetite-crystal growth in this experiment was performed using the Ostwald ripening model. This model mostly corresponds to the process of nanoparticle crystal growth because Ostwald ripening phenomenon commonly occur in the formation stage of crystals. Other models, such as oriented attachment, are commonly used to describe the phenomenon of crystal growth in the early stages of nucleation, in which the particle size doubles or multiplies from the initial particles (Huang et al., 2003). In addition, oriented attachment models are used to describe the peculiarities of non-classical growth and manufacturing anisotropic nanostructures, such as nanorods or nanowires (Zhang et al., 2010).

The general formula of Ostwald ripening is $r - r_0 = Kt^{1/n}$, where t is time, k is a temperature-dependent material constant appropriate to the value of the exponent n, and r_0 is the average particle radius at $t = 0$. When the exponent $n = 2$, it implies that crystal growth is controlled by the diffusion of ions along the matrix-particle boundary; when $n = 3$, the growth is controlled by the volume diffusion of ions in the matrix; and when $n = 4$, it indicates that growth is controlled by dissolution kinetics at the particle-matrix interface (Huang et al., 2003).

From the XRD data, the particle size (r) can be determined with the Scherrer formula (Equation 8). However, in this experiment we use a modification of the Scherrer formula (Equation 9) to minimize systematic errors from applying the original Scherrer formula (Monshi et al., 2012).

$$\beta = \frac{K\lambda}{D.\cos\theta} = \frac{K\lambda}{D}.\frac{1}{\cos\theta} \tag{8}$$

$$ln\beta = ln\frac{K\lambda}{D.\cos\theta} = ln\frac{K\lambda}{D} + ln\frac{1}{\cos\theta} \tag{9}$$

Matching the model is done using two approaches: (1) determining n and k with the least squares method; and (2) matching the experiment's curve of time versus radius with the theoretical curve. Based on the least squares method, the n and k values are shown in Table 2.

Table 2 The data resulting from the least squares method

R^2	ln K	1/n	k	n
0.947	1.67	0.27	5.31	3.66

From the data in Table 2, where the *n* value is 3.66 ≈ 4, this indicates that the crystal-growth reaction is controlled by dissolution kinetics at the particle-matrix interface. Even though the R^2 value shows good linearity, to be confident about the information, the experiment's curves are fitted to a theoretical curve, as depicted in Figure 6. The percentage errors are displayed in Table 3.

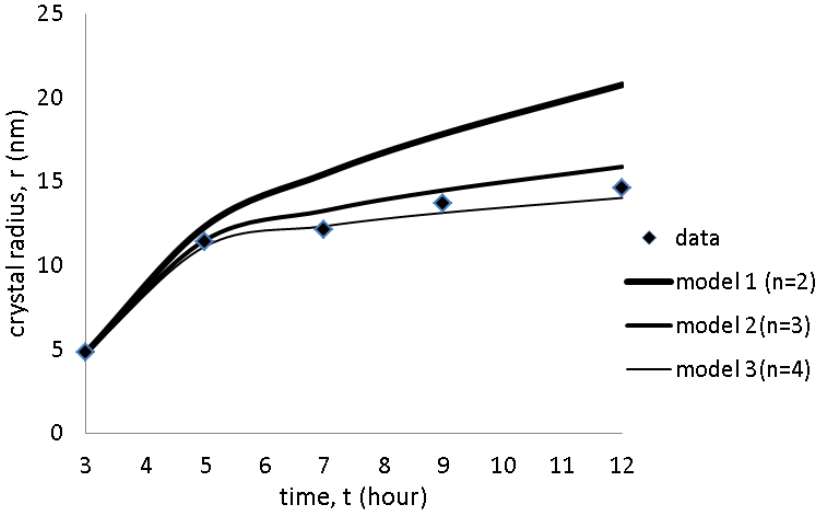

Figure 6 The graph of time vs. radius of nanomagnetite

Table 3 Percentage errors of experimental data to the model

Model	% Error
Model 1 (n=2)	20.44
Model 2 (n=3)	5.69
Model 3 (n=4)	2.53

Figure 6 reveals that there was an increase in the radius of magnetite crystals as time increased. Particles with a diameter of 4.8 nm were obtained after 3 hours of synthesis time. Whereas, from 7 hours to 12 hours, there was no significant size increase; the particles only grew by about 1 nm. Finally, after 12 hours of synthesis, nanoparticles with a radius of 14.6 nm were obtained. Each model provides an erratum that is quite different to the other models, with a certain tendency to be similar to the data from the experiment. The errors decrease in line with an increasing value of n. Model 3, which has a value of n = 4, is the closest to the data from the experiment with the lowest % error of 2.53% (Table 3). This indicates that, at a 220^{o}C temperature, nanomagnetite crystal growth follows the Ostwald ripening model controlled by the dissolution rate of the particle-matrix interface. With this model, we can predict the crystal size of magnetite nanoparticles in the reactor as a function of time and more easily control the size to suit the needs of the applications of the particles.

4. CONCLUSION

In conclusion, we have developed a facile, one-pot hydrothermal method for the synthesis of magnetite nanoparticles with a core-shell structure. The magnetite nanoparticles we obtained have monodispersity, no agglomeration, and a diameter of 50–60 nm. The magnetite nanoparticles also exhibited superparamagnetic properties, high saturation magnetization (65 emu/g), and were highly water soluble, which makes them an ideal candidate for drug delivery. The crystal growth kinetics study discovered a correlation among reaction time, crystal size, crystallinity, and magnetization saturation. A longer reaction time will increase the crystals' sizes and crystallinity. In addition, the value of the saturation magnetization grew with increasing crystallinity. The magnetite-crystal growth data can be fitted to an Ostwald ripening model with the growth being controlled by the dissolution of the surface reaction ($n \approx 4$), with a percentage error of 2.53%.

5. ACKNOWLEDGEMENT

Financial support for this study was provided by the Ministry of Research, Technology and Higher Education of the Republic of Indonesia (Kemenristekdikti).

6. REFERENCES

Arruebo, M., Pacheco, F.R., Ibarra, R.M., Santamaría, J., 2007. Magnetics Nanoparticles for Drug Delivery. *Nanotoday*, Volume 2(3), pp. 22–32

Bae, H.Y., Park, K., 2011. Targeted Drug Delivery to Tumors: Myths, Reality and Possibility. *Journal of Control Release*, Volume 153, pp. 198–205

Cao, X., Zhang, B., Zhao, F., Feng, L., 2012. Synthesis and Properties of MPEG-Coated Superparamagnetic Magnetite Nanoparticles. *Journal of Nanomaterials*, Volume 607296, pp. 1–6

Cheng, W., Tang, K., Qi, Y., Sheng, J., Liu, Z., 2010. One-step Synthesis of Superparamagnetic Monodisperse Porous Fe_3O_4 Hollow. *Journal of Material Chemistry*, Volume 2, pp. 1799–1805

Fitriana, N.K., Hafizah, E.A.M., Manaf, A., 2017. Synthesis and Magnetic Characterization of Mn-Ti Substituted $Sr0.6Fe_{2-x}Mn_{x/2}Ti_{x/2}O_3$ (x= 0.0-1.0) Nanoparticles by Combined Destruction Process. *International Journal of Technology*, Volume 8(4), pp. 644–650

Huang, F., Zhang, H., Banfield, F.J., 2003. Two-stage Crystal-growth Kinetics Observed during Hydhrothermal Coarsening of Nanocrystalline ZnS. *Nano Letters*, Volume 3, pp. 373–378

Hwang, N.M., Jung, S.J., Lee, K.D., 2012. *Thermodynamics – Fundamentals and Its Application in Science: Chapter 14: Thermodynamics and Kinetics in the Synthesis of Monodisperse Nanoparticles*, Korea, National Research Foundation of Korea (NRF)

International Union against Cancer (IUCC), 2009. 48th ICCA Congress & Exhibition Monday 9 November 2009, Available online at http://www.iccaworld.com/, Accessed on 5 April 2016

Khalil, M., Liu, N., Lee, L.R., 2017. Synthesis and Characterization of Hematite Nanoparticles using Ultrasonic Sonochemistry Method. *International Journal of Technology*, Volume 8(4), pp. 582–590

Luszczyk, K., Kaleta, J., Mech, R., 2014. Magnetic Core-shell Structures as Potential Carriers in Drug Delivery System. *International Journal of Engineering Science*, Volume 1, pp. 1–4

Marolt, M, 2014. Superparamagnetic Materials. *In*: Proceeding of Seminar I_b-4th Year (Old Program), University of Ljubljana Faculty of Mathematics and Physics 2014. Kranj, 23 April

Mohapatra, M., Anand, S., 2010. Synthesis and Applications of Nano-structured Iron Oxides/hydroxides – A Review. *International Journal of Engineering, Science and Technology*, Volume 2(8), pp. 127–146

Monshi, A., Foroughi, M.R, Monshi, M.R., 2012. Modified Scherrer Equation to Estimate More Accurately Nano-crystallite Size using XRD. *Journal of Nano Science and Engineering*, Volume 2, pp. 154–160

Qiao, R., Yang, C., Gao, M., 2009. Superparamagnetic Iron Oxide Nanoparticles: from Preparations to In Vivo MRI Applications. *Journal of Material Chemistry*, Volume 19, pp. 6274–6293

Thanh, N.T., K., Maclean, N., Mahiddine, S., 2014. Mechanisms of Nucleation and Growth of Nanoparticles in Solution. *American Chemical Society: Chemical Reviews*, Volume 114, pp. 7610−7630

Yu, M., Huang, S., Yu, K.J., Clyne, A.M., 2012. Dextran and Polymer Polyethylene Glycol (PEG) Coating Reduce Both 5 and 30 nm Iron Oxide Nanoparticle Cytotoxicity in 2D and 3D Cell Culture. *International Journal of Molecular Science*, Volume 13, pp. 5554–5570

Zhang, J., Hang, F., Lin, Z., 2010. Progress of Nanocrystalline Growth based on Oriented Attachment. *The Royal Society of Chemistry: Nanoscale*, Volume 2, pp. 18–34